

# Combined Effects of Ion-Pairing on Multi-Emissive Properties of Benzimidazolium Salts

Gabriele Di Carlo,<sup>\*[a]</sup> Alessandra Forni,<sup>\*[b]</sup> Paola Moretti,<sup>[a]</sup> Daniele Marinotto,<sup>[b]</sup> Chiara Botta,<sup>[c]</sup> Maddalena Pizzotti,<sup>[a]</sup> Francesca Tessore<sup>[a]</sup> and Elena Cariati<sup>[a]</sup>

[a] Prof. E. Cariati, Prof. F. Tessore, Prof. M. Pizzotti, Dr. G. Di Carlo and Mrs. P. Moretti  
Department of Chemistry  
University of Milan and INSTM Research Unit  
Via C. Golgi 19, 20133 Milan (Italy)  
E-mail: [gabriele.dicarlo@unimi.it](mailto:gabriele.dicarlo@unimi.it)

[b] Dr. A. Forni and Dr. D. Marinotto  
CNR-SCITEC, Istituto di Scienze e Tecnologie Chimiche "G. Natta"  
Via C. Golgi 19, 20133 Milan (Italy)  
E-mail: [alessandra.forni@scitec.cnr.it](mailto:alessandra.forni@scitec.cnr.it)

[c] Dr. Chiara Botta  
CNR-SCITEC, Istituto di Scienze e Tecnologie Chimiche "G. Natta"  
Via A. Corti 12, 20133 MILANO (Italy)

## Table of Contents

1	Experimental details .....	1
1.1	General information .....	1
1.2	Synthesis.....	1
1.3	Single crystal X-ray crystallographic studies.....	1
1.4	Computational details .....	2
1.5	Photophysical characterization .....	2
2	NMR studies .....	3
3	Photophysical Studies.....	6
3.1	Solutions .....	6
3.2	Solids.....	8
4	Crystal structures.....	11
5	Theoretical studies .....	13
6	References .....	20

## 1 Experimental details

### 1.1 General information

All reagents and solvents involved in the synthesis were purchased from Sigma Aldrich and used as received, except THF (freshly distilled from Na/benzophenone under nitrogen atmosphere). Glassware has been flame-dried under vacuum before use when necessary.  $^1\text{H}$ -NMR spectra were recorded on a Bruker Avance DRX-400 in  $\text{DMSO}-d_6$ ,  $\text{CDCl}_3$  and  $\text{CD}_3\text{OD}$  as solvents at  $10^{-3}\text{M}$  ( $10^{-5}\text{M}$  where shown). Elemental analysis was carried out with a Perkin-Elmer CHN 2400 instrument.

### 1.2 Synthesis

Triflate (**1-OTf**), nitrate (**1-NO<sub>3</sub>**) and Iodide (**1-I**) salts of 1,3-dimethyl-2-(4-methylphenyl)-1H-benzimidazolium (**1**) are easily obtained by following the synthetic strategy previously reported by some of us.[S1] The high purity grade of the final products, required for photophysical measurements, are obtained by Biotage flash chromatography and multiple recrystallizations with proper solvents.

**1-OTf crystals** were obtained by repeated crystallization steps from ethanol at +4°C. Elemental analysis calcd (%) for  $\text{C}_{17}\text{H}_{17}\text{F}_3\text{N}_2\text{O}_3\text{S}$ : C 52.84, H 4.43, N 7.25; found C 52.71, H 4.43, N 7.24. MS-ESI (+) m/z: calcd (%) for  $\text{C}_{16}\text{H}_{17}\text{N}_2^+$  237, found 237 [M]<sup>+</sup>. MS-ESI (-) m/z: calcd (%) for  $\text{CF}_3\text{O}_3\text{S}^-$  149, found 149 [M]<sup>-</sup>.

**1-NO<sub>3</sub>·0.5EtOH crystals** were obtained by repeated crystallization steps from ethanol at +4°C. Elemental analysis calcd (%) for  $\text{C}_{16}\text{H}_{17}\text{N}_3\text{O}_3$ : C 63.34, H 6.25, N 13.04; found C 63.18, H 6.23, N 13.08. MS-ESI (+) m/z: calcd (%) for  $\text{C}_{16}\text{H}_{17}\text{N}_2^+$  237, found 237 [M]<sup>+</sup>. MS-ESI (-) m/z: calcd (%) for  $\text{NO}_3^-$  62, found 62 [M]<sup>-</sup>.

**1-NO<sub>3</sub>·H<sub>2</sub>O crystals** were obtained by repeated crystallization steps from acetonitrile/water (9:1) solution at +4°C. Elemental analysis calcd (%) for  $\text{C}_{16}\text{H}_{19}\text{N}_3\text{O}_4 \cdot [0.5\text{C}_2\text{H}_6\text{O}]$ : C 60.56, H 6.03, N 13.24; found C 60.47, H 6.01, N 13.21. MS-ESI (+) m/z: calcd (%) for  $\text{C}_{16}\text{H}_{17}\text{N}_2^+$  237, found 237 [M]<sup>+</sup>. MS-ESI (-) m/z: calcd (%) for  $\text{NO}_3^-$  62, found 62 [M]<sup>-</sup>.

**1-I·0.5CH<sub>2</sub>Cl<sub>2</sub> crystals** were obtained by repeated crystallization steps from dichloromethane at +4°C. Elemental analysis calcd (%) for  $\text{C}_{16}\text{H}_{17}\text{IN}_2 \cdot [0.5\text{CH}_2\text{Cl}_2]$ : C 48.73, H 4.46, N 6.89; found C 48.87, H 4.46, N 6.90. MS-ESI (+) m/z: calcd (%) for  $\text{C}_{16}\text{H}_{17}\text{N}_2^+$  237, found 237 [M]<sup>+</sup>. MS-ESI (-) m/z: calcd (%) for I<sup>-</sup> 127, found 127 [M]<sup>-</sup>.

### 1.3 Single crystal X-ray crystallographic studies

X-ray data of **1-OTf**, **1-NO<sub>3</sub>·0.5EtOH**, **1-NO<sub>3</sub>·H<sub>2</sub>O** and **1-I·0.5CH<sub>2</sub>Cl<sub>2</sub>** were collected on a Bruker Apex II diffractometer using MoK $\alpha$  radiation. The structures were solved using direct methods and refined using a full-matrix least squares procedure based on F<sup>2</sup> using all data [S2]. Hydrogen atoms were

placed at geometrically estimated positions. Details relating to the crystals and the structural refinements are presented in Table S2. Full details of crystal data and structure refinement, in CIF format, are available as Supplementary Information.

CCDC reference numbers: 2018732 (**1-OTf**), 2018733 (**1-NO<sub>3</sub>·0.5EtOH**), 2018734 (**1-NO<sub>3</sub>·H<sub>2</sub>O**) and 2018735 (**1-I·0.5CH<sub>2</sub>Cl<sub>2</sub>**).

#### 1.4 Computational details

DFT and TDDFT calculations have been performed in vacuo at the ωB97X/6-311++G(d,p) level of theory on both the 1,3-dimethyl-2-(4-methylphenyl)-1H-benzimidazolium cation **1** and its salts with OTf<sup>-</sup>, NO<sub>3</sub><sup>-</sup> and I<sup>-</sup> anions. The ωB97X [S3] functional was used owing to its ability in correctly treating at the same time not only ground and excited states properties, but also intermolecular interactions. In the case of the free cation, geometry was fully optimized starting from the X-ray one of **1-OTf**. As for the salts, the cation-anion pairs displaying the shortest intermolecular contacts in the corresponding X-ray structures have been extracted from the crystal and submitted to geometry optimization by constraining angles and torsions to the experimental values.

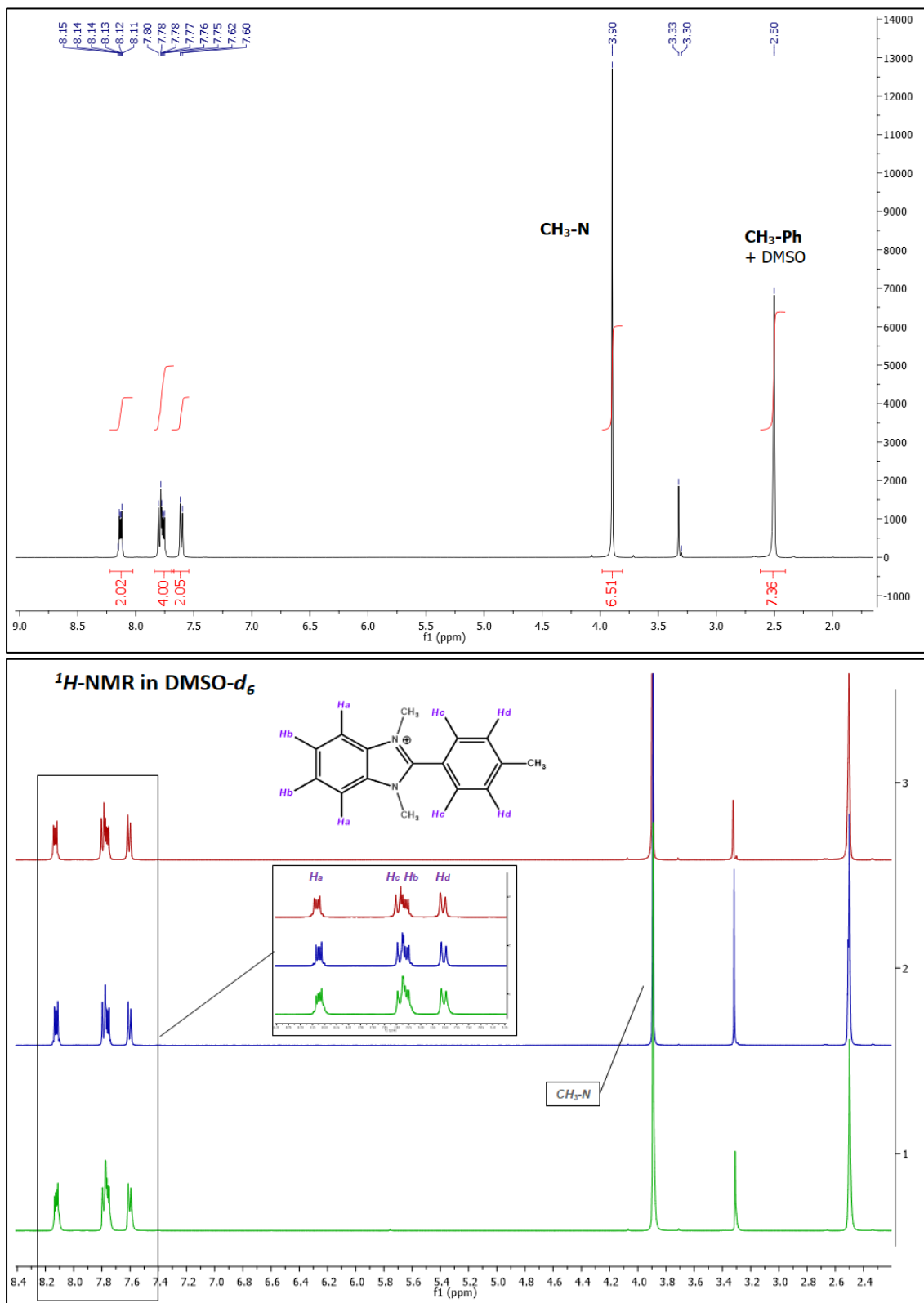
All calculations have been performed with the Gaussian 16 program (Revision A.03) [S4].

#### 1.5 Photophysical characterization

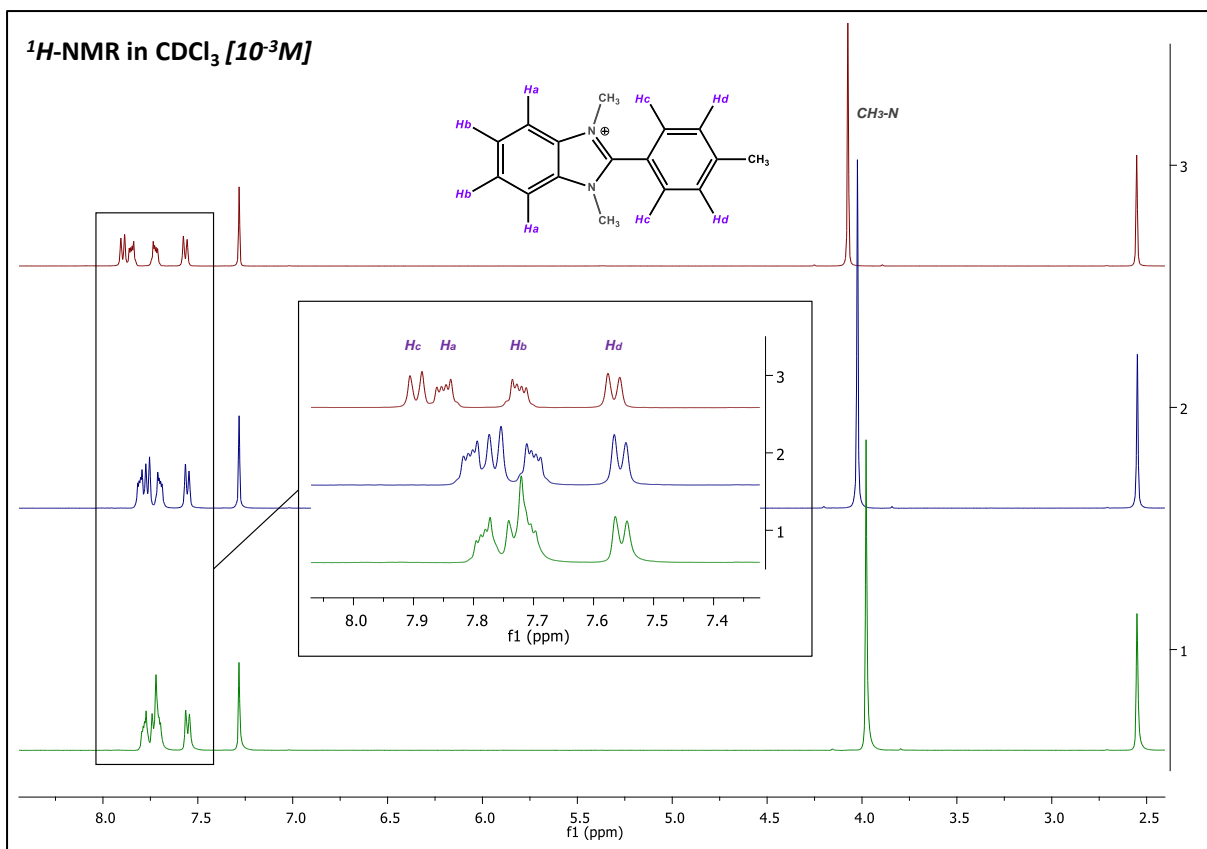
Luminescence measurements. Steady state emission and excitation spectra and photoluminescence lifetimes were obtained using a FLS 980 spectrofluorimeter (Edinburgh Instrument Ltd). The steady state measurements were obtained by a 450 W Xenon arc lamp. Photoluminescence lifetime measurements were performed using: Edinburgh EPLED-300, (Edinburgh Instrument Ltd) and microsecond flash Xe-lamp (60W, 0.1÷100 Hz) with data acquisition devices time correlated single-photon counting (TCSPC) and multi-channel scaling (MCS) methods, respectively.

Photoluminescence quantum yields were measured using a C11347 Quantaurus – Absolute Photoluminescence Quantum Yield Spectrometer (Hamamatsu Photonics K.K), equipped with a 150 W Xenon lamp, an integrating sphere and a multichannel detector.

## 2 NMR studies



**Figure S1:** Integrated  $^1\text{H}$ -NMR spectrum (up) of **1-I** (at 298K) in  $\text{DMSO}-d_6$ . Stacked  $^1\text{H}$ -NMR spectra (down) of **1-I** (red); **1-NO<sub>3</sub>** (blue); **1-OTf** (green).



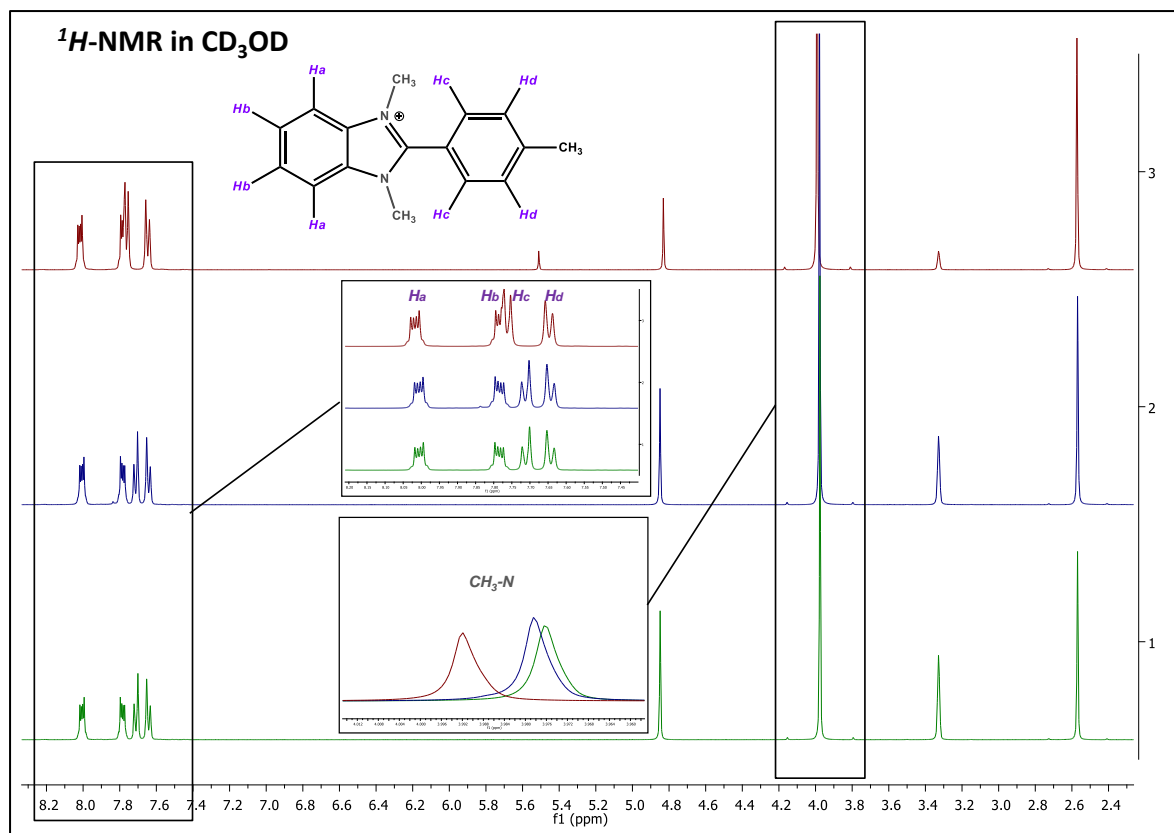


**Figure S3.** Stacked  $^1H$ -NMR spectra (at 298K) in  $CD_3OD$  of **1-I** (red); **1-NO<sub>3</sub>** (blue); **1-OTf** (green).

### 3 Photophysical Studies

#### 3.1 Solutions

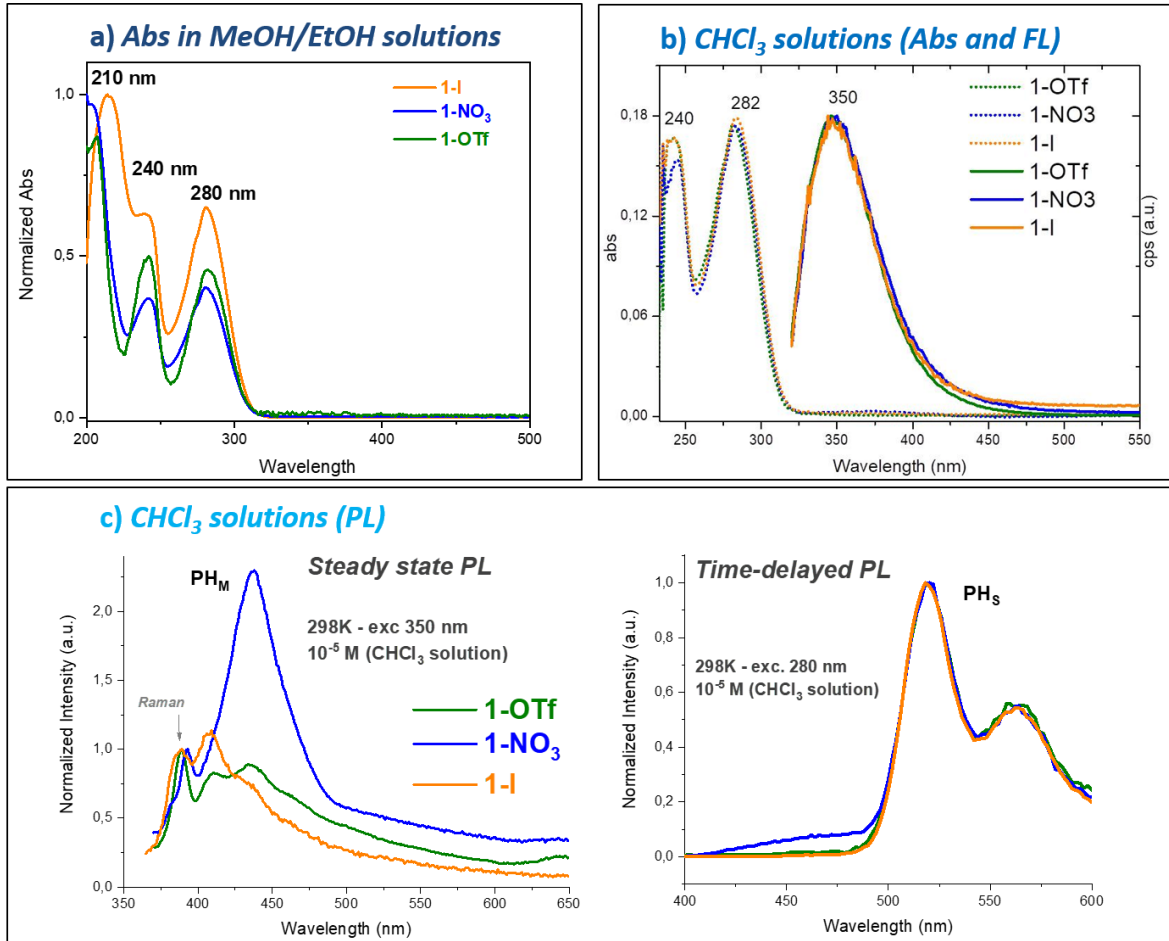
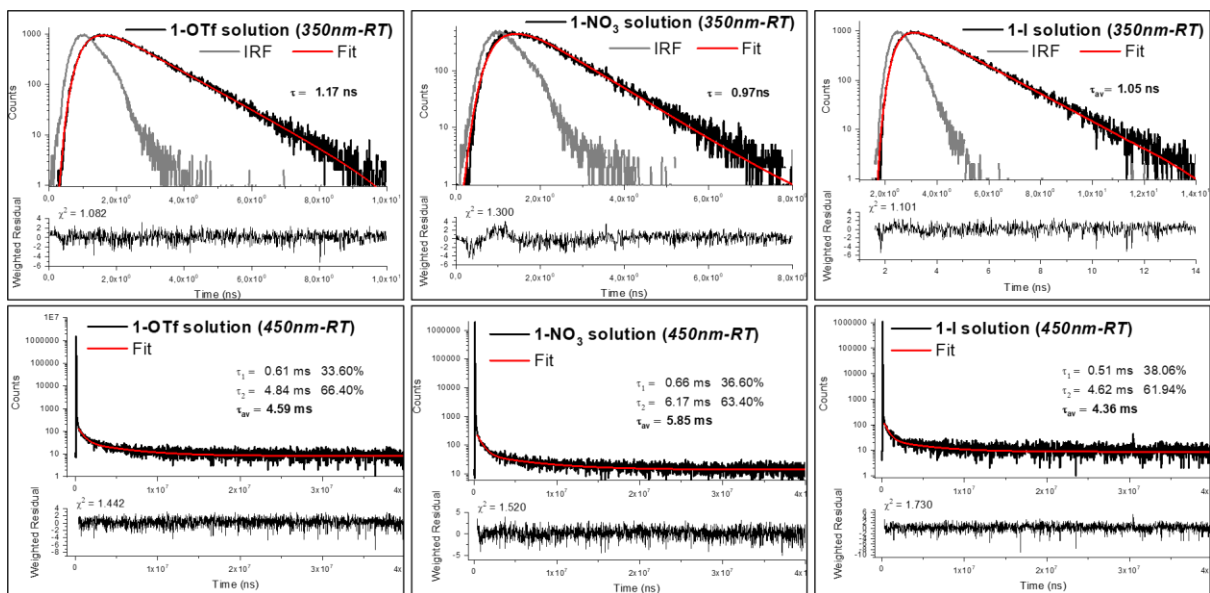
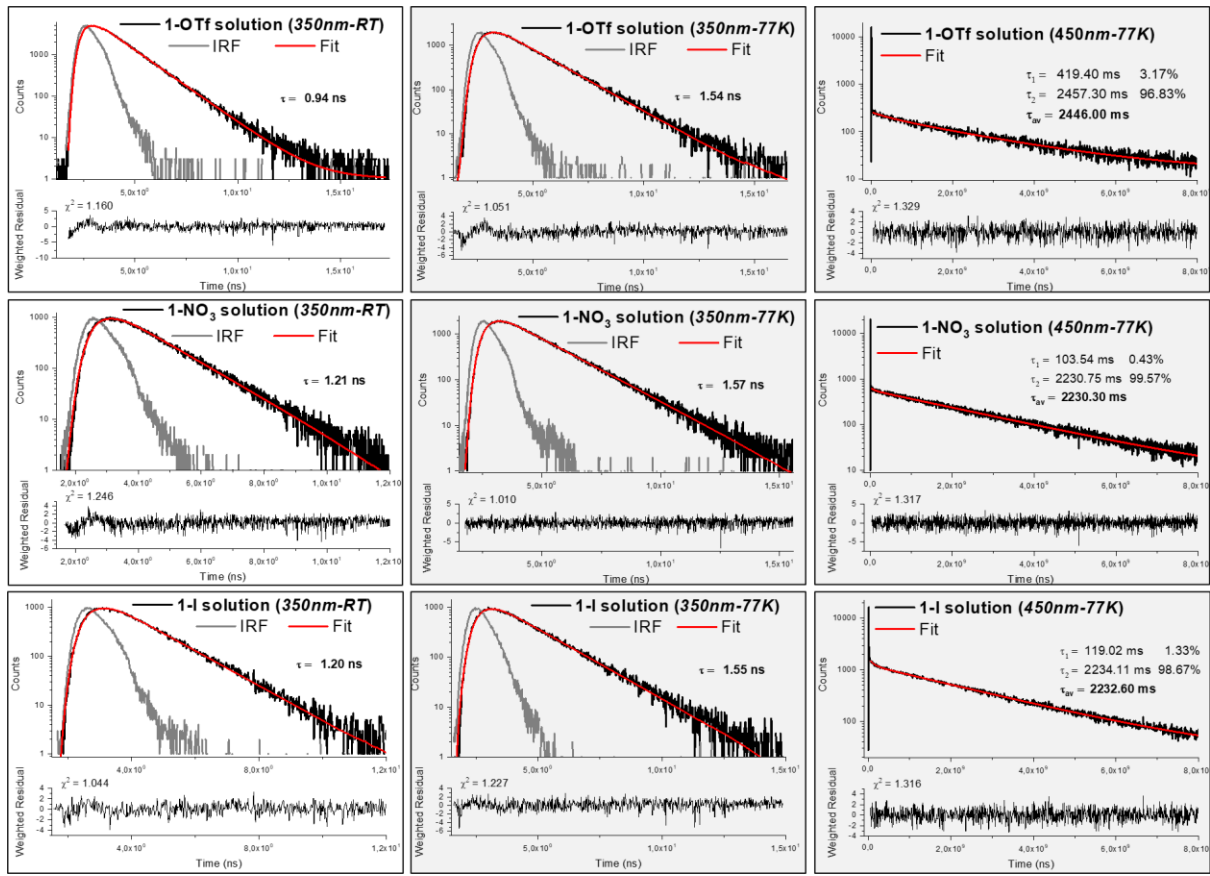


**Figure S4.** a) Absorption spectrum of diluted solutions ( $10^{-5}$  M) of **1**-salts in MeOH/EtOH. b) Absorption (solid line) and emission spectra (dotted line; exc 300 nm) at RT of diluted solutions ( $10^{-5}$  M) of **1**-salts in CHCl<sub>3</sub>. c) Steady-state and time-delayed PL emission spectra of **1**-salts in CHCl<sub>3</sub> (delay time 0.2 ms and window 1.5 ms for **1-OTf** and **1-I**; delay time 0.1 ms and window 0.5 ms for **1-NO<sub>3</sub>**).



### 3.2 Solids

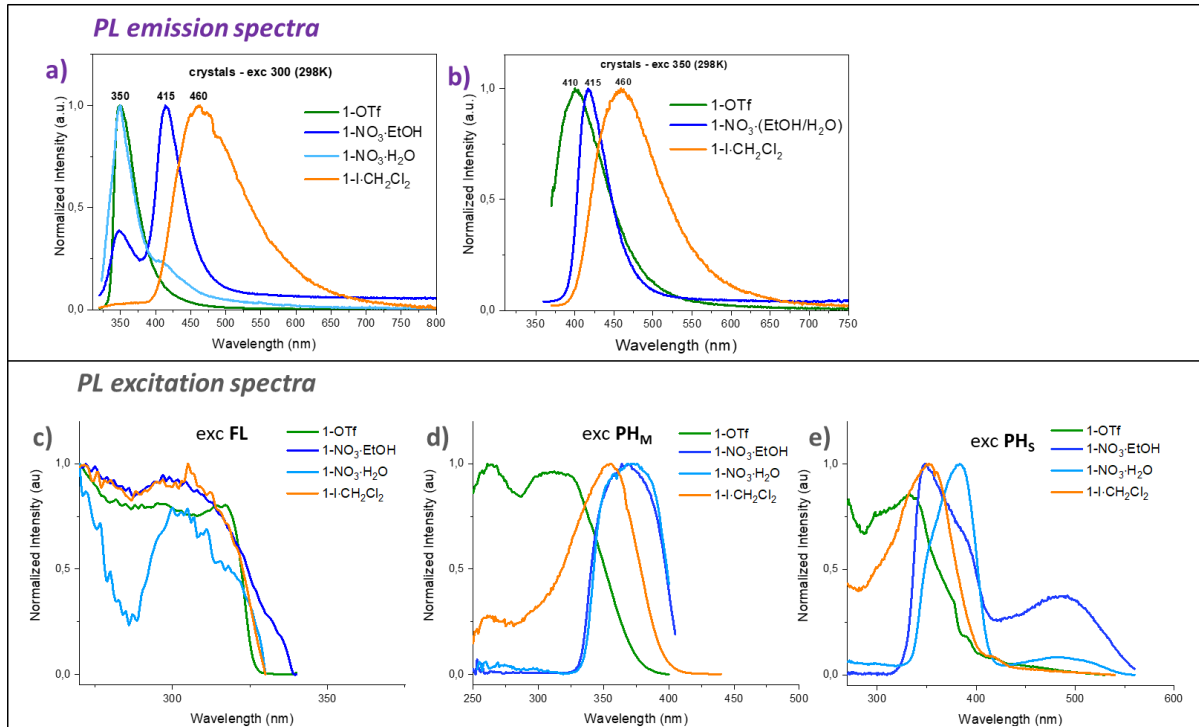


**Figure S7.** a) PL emission spectra of **1-OTf**, **1-NO<sub>3</sub>-EtOH**, **1-NO<sub>3</sub>-H<sub>2</sub>O** and **1-I-CH<sub>2</sub>Cl<sub>2</sub>** crystals at 298K (300 nm excitation). b) PL emission spectra at 298K under 350 nm excitation. c) Fluorescence excitation spectra. d) Molecular Phosphorescence excitation spectra. e) Supramolecular Phosphorescence excitation spectra.

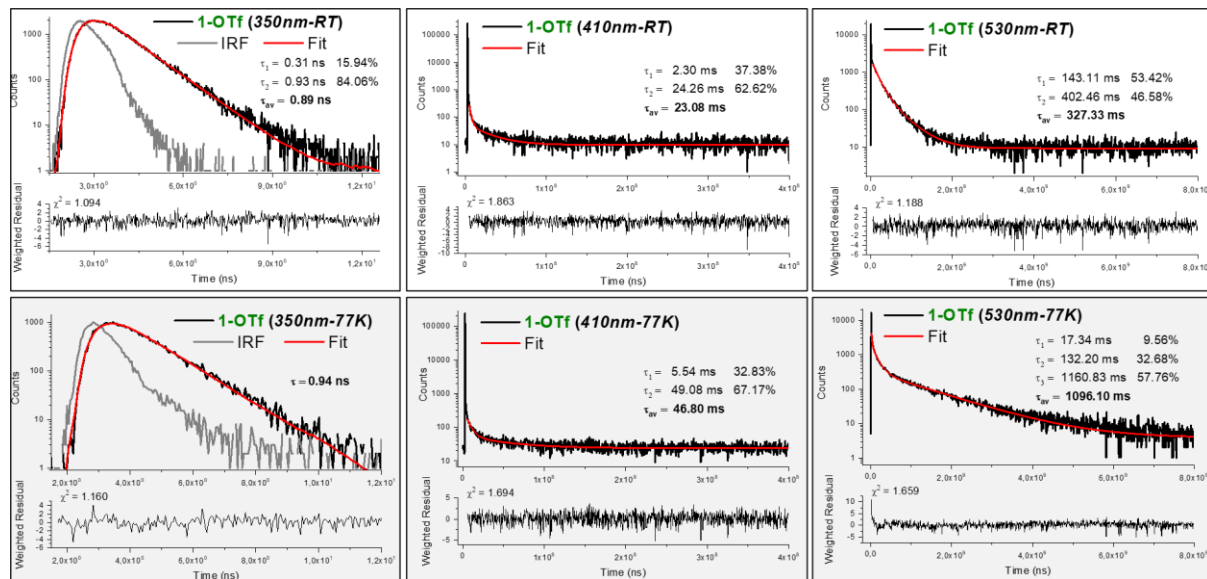


**Figure S8.** FL (350 nm), PH<sub>M</sub> (410 nm) and PH<sub>S</sub> (530 nm) decay profiles of **1-OTf** crystals (excitation 300 nm).

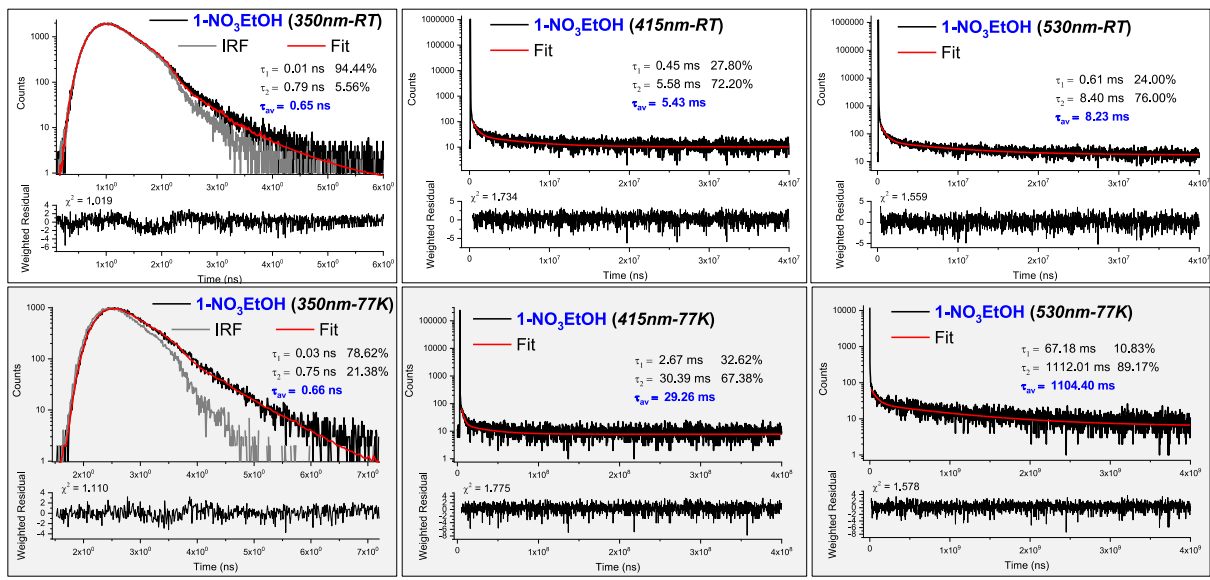


**Figure S9.** FL (350 nm), PH<sub>M</sub> (415 nm) and PH<sub>S</sub> (530 nm) decay profiles of **1-NO<sub>3</sub>-EtOH** crystals (excitation 300 nm).

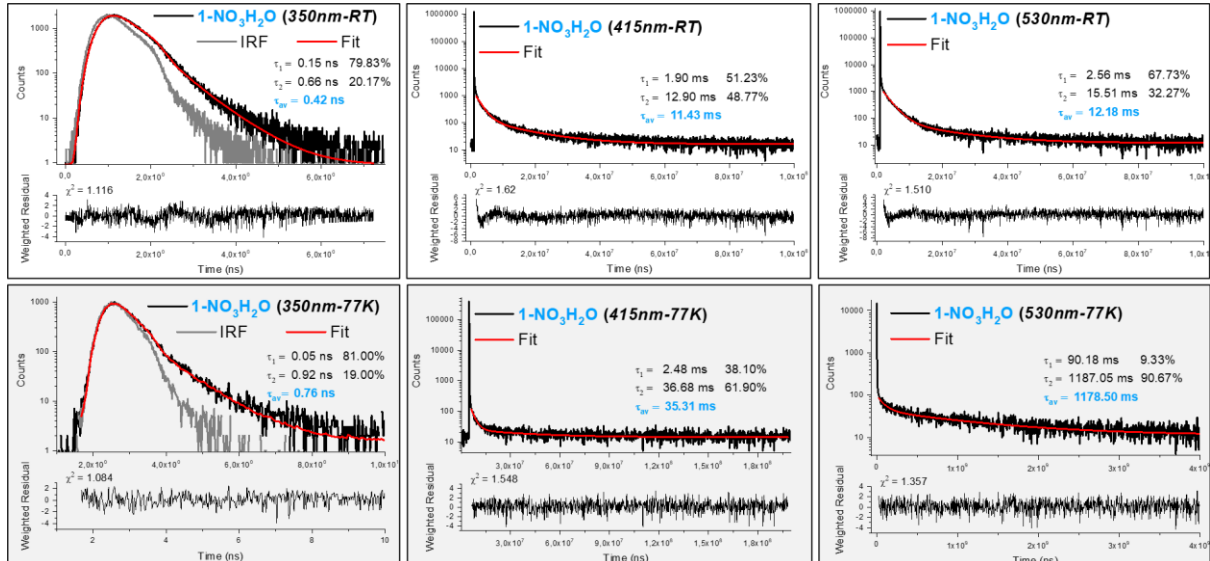


**Figure S10.** FL (350 nm), PH<sub>M</sub> (415 nm) and PH<sub>S</sub> (530 nm) decay profiles of **1-NO<sub>3</sub>-H<sub>2</sub>O** crystals (excitation 300 nm).

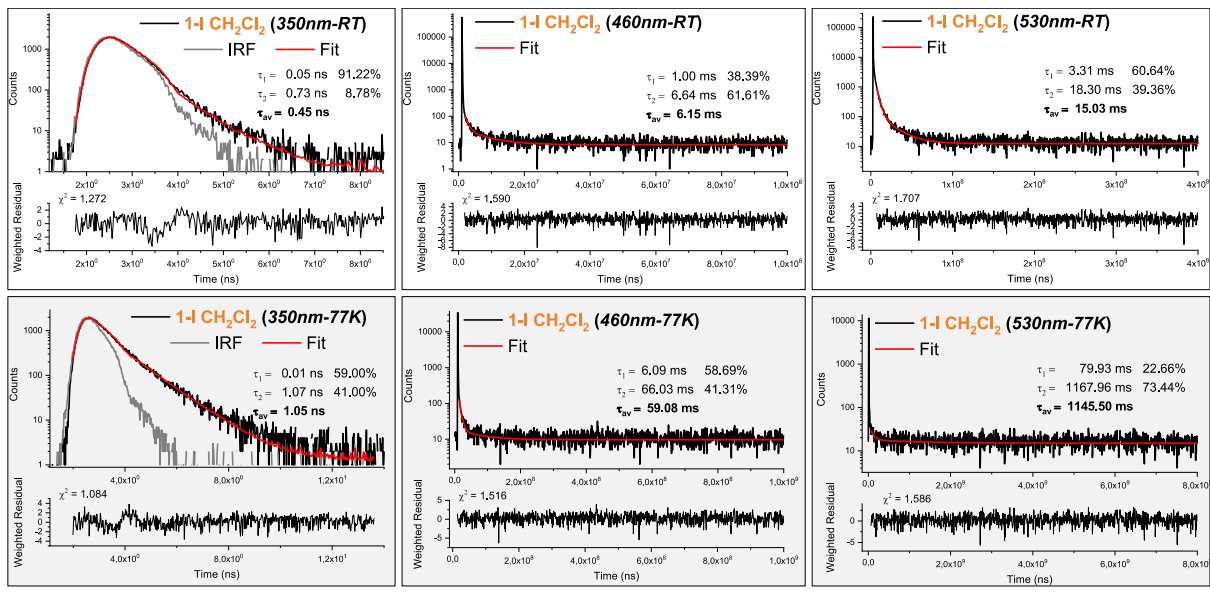


**Figure S11.** FL (350 nm), PH<sub>M</sub> (460 nm) and PH<sub>S</sub> (530 nm) decay profiles of **1-I·CH<sub>2</sub>Cl<sub>2</sub>** crystals (excitation 300 nm).

**Table S1.** Radiative ( $K_r$ ) and non-radiative ( $K_{nr}$ ) constants of **1**-salts.

		$\phi$	$\tau$ (ns)	$K_r(s^{-1})^a$	$K_{nr}(s^{-1})^b$	$K_r/K_{nr}$
<b>1-Otf</b> <i>MeOH/EtOH</i>	<i>Em350</i> (exc300)	0,775	0,94	<b>8,24E+08</b>	<b>2,39E+08</b>	<b>3,45</b>
<b>1-Otf</b> <i>crystal</i>	<i>Em350</i> (exc300)	0,507	0,89	<b>5,69E+08</b>	<b>5,54E+08</b>	<b>1,03</b>
	<i>Em410</i> (exc350)	0,347	2,3E+07	<b>15,0870</b>	<b>28,3913</b>	<b>0,53</b>
<b>1-NO<sub>3</sub></b> <i>MeOH/EtOH</i>	<i>Em350</i> (exc300)	0,526	1,21	<b>4,35E+08</b>	<b>3,92E+08</b>	<b>1,11</b>
<b>1-NO<sub>3</sub>·EtOH</b> <i>crystal</i>	<i>Em350</i> (exc300)	0,037	0,65	<b>5,69E+07</b>	<b>1,48E+09</b>	<b>0,04</b>
	<i>Em410</i> (exc350)	0,73	5,4E+06	<b>135,1852</b>	<b>50,0000</b>	<b>2,70</b>
<b>1-NO<sub>3</sub>·H<sub>2</sub>O</b> <i>crystal</i>	<i>Em350</i> (exc300)	0,019	0,42	<b>4,52+07</b>	<b>2,34E+09</b>	<b>0,02</b>
	<i>Em410</i> (exc350)	0,25	1,14E+07	<b>21,8532</b>	<b>65,5594</b>	<b>0,33</b>
<b>1-I</b> <i>MeOH/EtOH</i>	<i>Em350</i> (exc300)	0,536	1,20	<b>4,47E+08</b>	<b>3,87E+08</b>	<b>1,16</b>
<b>1-I·CH<sub>2</sub>Cl<sub>2</sub></b> <i>crystal</i>	<i>Em350</i> (exc300)	0,114	0,45	<b>2,53E+08</b>	<b>1,97E+09</b>	<b>0,13</b>
	<i>Em410</i> (exc350)	0,237	6,15E+06	<b>38,5366</b>	<b>124,0650</b>	<b>0,31</b>

$$^a K_r = \phi \cdot \tau^{-1}$$

$$^b K_{nr} = K_r \cdot (\phi^{-1} - 1)$$

## 4 Crystal structures

**Table S2.** Crystallographic data and structure refinement details for **1-OTf**, **1-NO<sub>3</sub>·0.5EtOH**, **1-NO<sub>3</sub>·H<sub>2</sub>O** and **1-I·0.5CH<sub>2</sub>Cl<sub>2</sub>**

	<b>1-OTf</b>	<b>1-NO<sub>3</sub>·0.5EtOH</b>	<b>1-NO<sub>3</sub>·H<sub>2</sub>O</b>	<b>1-I·0.5CH<sub>2</sub>Cl<sub>2</sub></b>
Chemical Formula	C <sub>16</sub> H <sub>17</sub> N <sub>2</sub> , CF <sub>3</sub> O <sub>3</sub> S	C <sub>16</sub> H <sub>17</sub> N <sub>2</sub> , NO <sub>3</sub> , 0.5(C <sub>2</sub> H <sub>6</sub> O)	C <sub>16</sub> H <sub>17</sub> N <sub>2</sub> , NO <sub>3</sub> , O	2(C <sub>16</sub> H <sub>17</sub> N <sub>2</sub> ), 2I, CH <sub>2</sub> Cl <sub>2</sub>
Molecular weight	386.38	322.36	315.32	813.36
T(K)	293(2)	120(2)	293(2)	120(2)
Crystal system	Triclinic	Monoclinic	Triclinic	Monoclinic
space group	P-1	C2/c	P-1	C2/c
a(Å)	7.5128(5)	46.7400(18)	7.456(2)	17.3639(9)
b(Å)	8.6916(5)	7.5898(3)	9.299(3)	7.5370(4)
c(Å)	13.7154(8)	28.5740(11)	12.571(3)	26.8262(14)
α(°)	104.2767(9)	90	75.967(4)	90
β(°)	91.5096(9)	106.8120(10)	77.518(4)	105.8189(7)
γ(°)	91.7180(9)	90	70.952(4)	90
V(Å <sup>3</sup> )	867.02(9)	9703.3(7)	790.3(4)	3377.8(3)
Z	2	24	2	4
D <sub>calcd</sub> (g cm <sup>-3</sup> )	1.480	1.324	1.325	1.599
μ (mm <sup>-1</sup> )	0.237	0.094	0.097	2.048
Crystal size (mm)	0.55 x 0.17 x 0.03	0.32 x 0.33 x 0.22	0.15 x 0.12 x 0.12	0.42 x 0.27 x 0.12
2θ <sub>max</sub> , °	61.04	61.03	61.13	61.02
No. of measured, independent and observed [I > 2σ(I)] reflections	19531 / 5294 / 3976	88189 / 14792 / 10977	14379 / 4815 / 2538	31951 / 5159 / 4935
(R <sub>int</sub> )/(R <sub>σ</sub> )	0.0202 / 0.0190	0.0341 / 0.0267	0.0322 / 0.0404	0.0140 / 0.0093
data/restraints/params	5294 / 0 / 238	14792 / 78 / 690	4811 / 0 / 211	5159 / 0 / 201
R[F <sup>2</sup> > 2σ(F <sup>2</sup> )], wR(F <sup>2</sup> )	0.0695, 0.1278	0.0503, 0.1503	0.0723, 0.2593	0.0187, 0.0482
S	1.055	1.035	1.025	1.067
Δρ <sub>max</sub> , Δρ <sub>min</sub> (e Å <sup>-3</sup> )	0.225, -0.355	0.417, -0.243	0.293, -0.432	0.913, -0.627

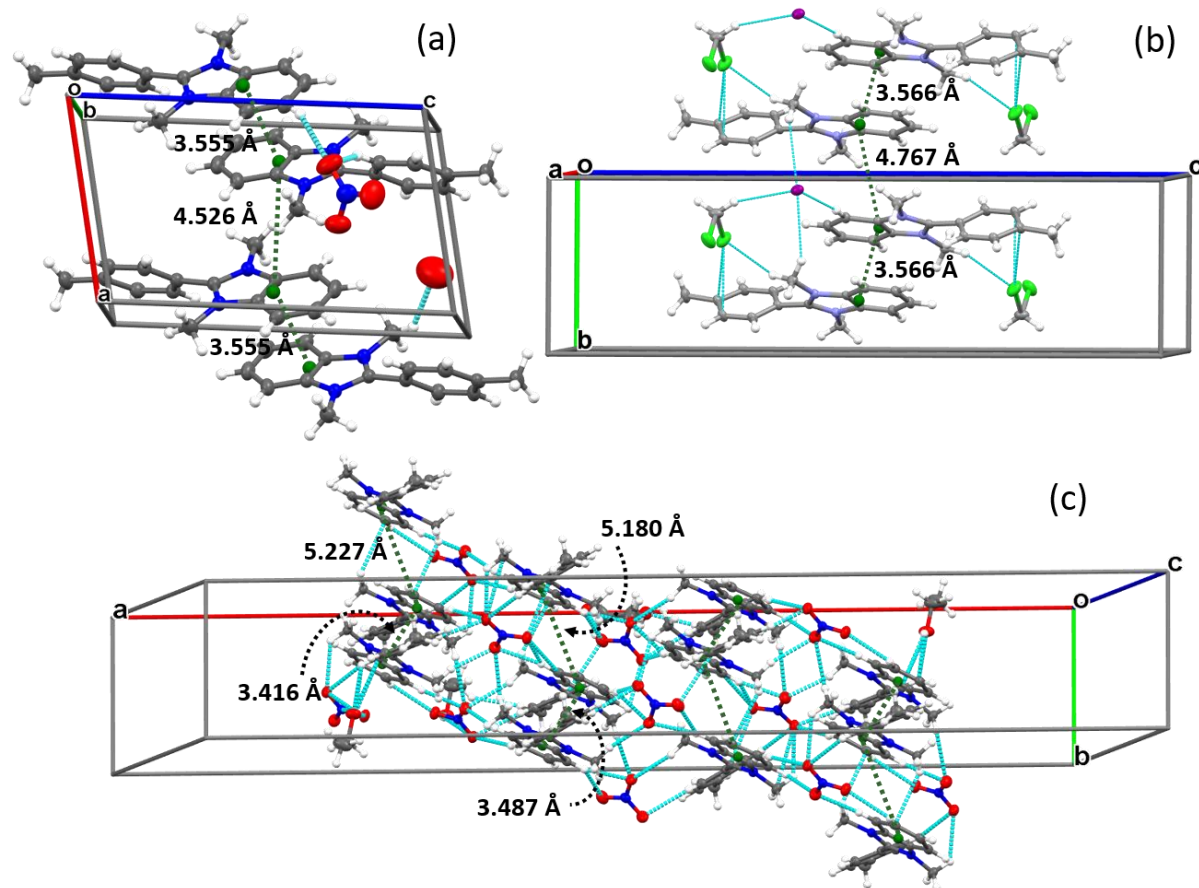


**Figure S12.** Fragments of crystal packing of (a) **1-NO<sub>3</sub>·H<sub>2</sub>O**, (b) **1-I·0.5CH<sub>2</sub>Cl<sub>2</sub>** and (c) **1-NO<sub>3</sub>·0.5EtOH** with contacts shorter than the sum of van der Waals radii (cyan dashed lines) and distances between benzimidazole centroids (green circles). Ellipsoids at 30% (**1-NO<sub>3</sub>·H<sub>2</sub>O**) and 50% (**1-I·0.5CH<sub>2</sub>Cl<sub>2</sub>** and **1-NO<sub>3</sub>·0.5EtOH**) probability.

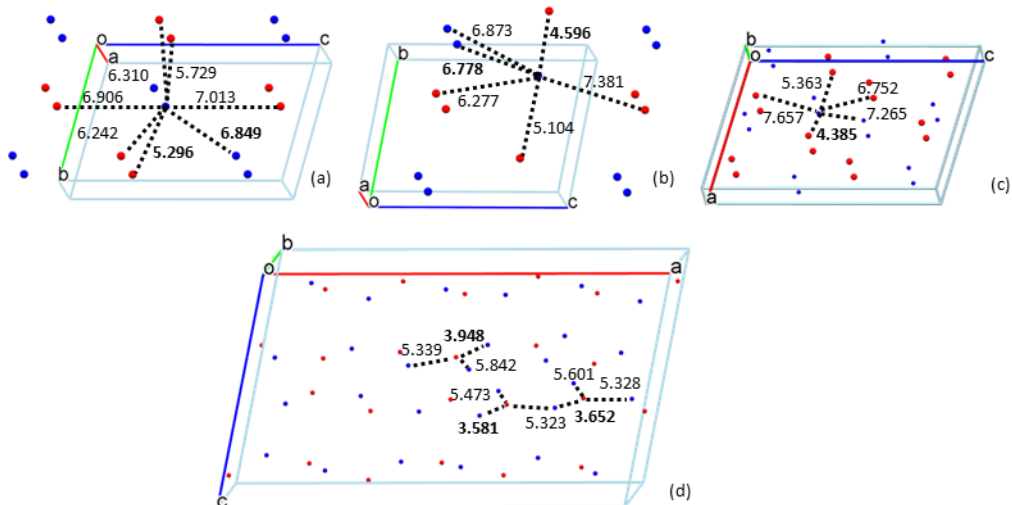


**Figure S13.** Shortest distances between cation and anion (blue and red circles, respectively) centroids in the crystal structures of (a) **1-OTf**, (b) **1-NO<sub>3</sub>·H<sub>2</sub>O**, (c) **1-I·0.5CH<sub>2</sub>Cl<sub>2</sub>** and (d) **1-NO<sub>3</sub>·0.5EtOH**.

## 5 Theoretical studies

Comparison between the optimized geometry of **1** in gas phase with the X-ray ones of the **1-OTf**, **1-NO<sub>3</sub>·0.5EtOH**, **1-NO<sub>3</sub>·H<sub>2</sub>O** and **1-I·0.5CH<sub>2</sub>Cl<sub>2</sub>** salts indicates that crystal packing does not perturb significantly the molecular conformation, which can be then supposed to be preserved also in solution. The optimized structure of **1** is in fact only slightly more twisted with respect to that found in the crystal structures, as indicated by the dihedral angle  $\theta$  between the I.s. planes through the benzimidazole moiety and the phenyl atoms. This angle measures in fact 59.92° in the optimized structure of **1** and 52.35° in the crystal structure of **1-OTf**, 48.23, 53.21 and 49.71° in the three independent molecules of **1-NO<sub>3</sub>·0.5EtOH**, 53.09° in **1-NO<sub>3</sub>·H<sub>2</sub>O** and 48.33° in **1-I·0.5CH<sub>2</sub>Cl<sub>2</sub>**. Moreover, the distance of the C9–C10 bond connecting the two aromatic moieties is comparable in all cases, varying from 1.462 to 1.469 Å, suggesting a similar conjugation degree in the isolated cation and in the salts.

The simulated absorption spectrum of **1** is reported in Figure S14 (see Table S3 for the first singlet and triplet excitation energies). The overall shape of the spectrum reproduces the experimental one in MeOH/EtOH (displaying three bands at 210, 240 and 280 nm), though the computed maxima (at 190, 220, 245 nm) are slightly shifted towards higher energies.

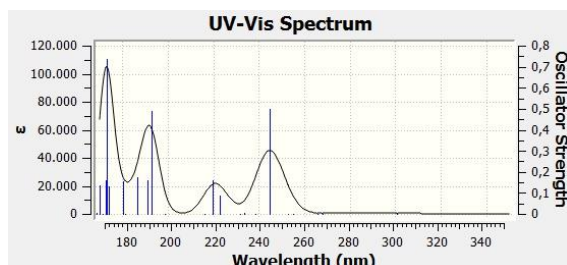


**Figure S14.** ωB97X/6-311++G(d,p) computed absorption spectrum of **1**, resulting from convolution of the excitation energies (blue sticks) with 0.15 eV of half-bandwidth

The  $S_0 \rightarrow S_1$  excitation, computed at 245 nm with oscillator strength  $f=0.60$ , is mainly (75%) a HOMO→LUMO transition where both HOMO and LUMO are  $\pi$  orbitals delocalized on the whole molecule (see Figure S15).

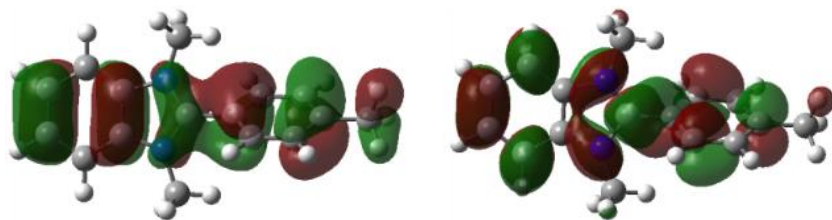


**Figure S15.** Plot of  $\omega$ B97X/6-311++G(d,p) HOMO (left) and LUMO (right) of the optimized geometry of **1** with an isosurface value of 0.02.

Analysis of the first singlet and triplet excitation energies (see Table S3) reveals the presence of a triplet state ( $T_1$ ) of ( $\pi,\pi^*$ ) character just below  $S_1$  ( $\Delta E=0.162$  eV, 8 nm). Such small S-T energy gap could allow an otherwise forbidden ISC from the singlet to the close triplet state which decays to  $T_1$  by internal conversion, explaining the fluorescent (from  $S_1$ ) and phosphorescent (from  $T_1$ ) emission of solutions of **1**-salts, the latter observed only at low temperature, as usually happen for typical organic molecules. The ( $\pi,\pi^*$ ) character of the emission from  $T_1$  to  $S_0$  explains its long lifetimes in solution.

Calculations of the excitation energies on the **1-OTf**, **1-NO<sub>3</sub>** and **1-I** ionic pairs to simulate any effect of the counterion on the emissive properties of **1** (see Table S4 for **1-OTf**) provide the first significantly populated (i.e. with  $f>0.1$ ) singlet excited state slightly shifted towards lower energies (248, 249 and 253 nm for **1-OTf**, **1-NO<sub>3</sub>** and **1-I**, respectively) with respect to **1**. Moreover, they display CT character from the anion towards **1** as exemplified in Figure S16 for **1-OTf**, where we plot the MOs mainly involved (66%) in the  $S_0 \rightarrow S_1$  transition.

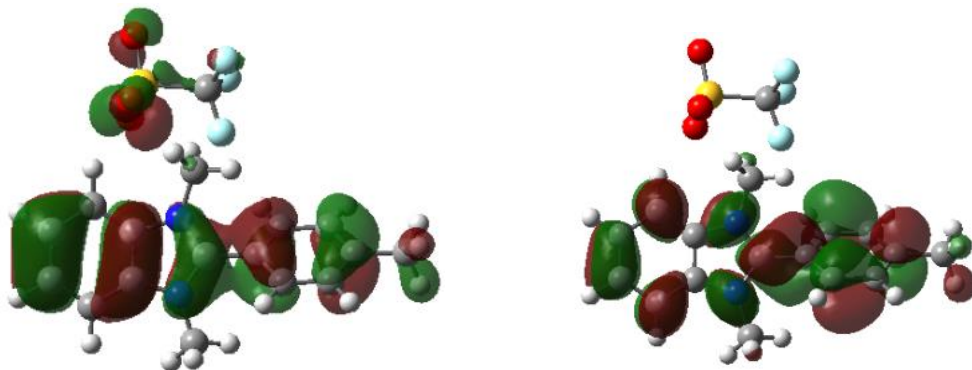


**Figure S16.** Plot of  $\omega$ B97X/6-311++G(d,p) occupied (left) and unoccupied (right) MOs mainly involved in the  $S_0 \rightarrow S_1$  transition of the **1-OTf** pair (isosurface value 0.02).

Optimization of  $S_1$  of **1** (see Figure S17 for the simulated spectrum of fluorescence) leads to a more planar conformation with respect to the ground state one (the dihedral angle  $\theta$  measures  $27.77^\circ$ ),

indicating a larger conjugation within the molecule. In fact, the C–C bond connecting the phenyl ring with benzimidazole shortens from 1.469 (ground state) to 1.402 Å (excited state). The fluorescence is computed at 312 nm with high oscillator strength ( $f=0.88$ ), in agreement with the high quantum yields measured in solution. The computed Stokes shift (about 70 nm) is comparable with the experimental one.

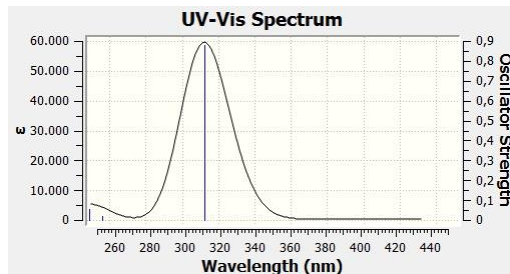


**Figure S17.** ωB97X/6-311++G(d,p) fluorescence spectrum of **1**, resulting from convolution of the excitation energies (blue sticks) with 0.2 eV of half-bandwidth

**Table S3.** First TD- $\omega$ B97X/6-311++G(d,p)  $S_0 \rightarrow S_n$  and  $S_0 \rightarrow T_n$  transitions computed on the optimized structure of **1**.

Excitation energies and oscillator strengths:

T1	Excited State	1:	Triplet-A	3.4468 eV	359.71 nm	f=nd	$\langle S^{**2} \rangle = 2.000$
	60 -> 64		0.15339				
	60 -> 66		-0.25298				
	61 -> 65		-0.34304				
	61 -> 68		0.10297				
	63 -> 64		0.39109				
	63 -> 66		-0.27116				
T2	Excited State	2:	Triplet-A	3.4953 eV	354.72 nm	f=nd	$\langle S^{**2} \rangle = 2.000$
	60 -> 68		-0.19525				
	62 -> 64		0.49892				
	62 -> 66		0.30488				
	62 -> 70		-0.15923				
	63 -> 68		0.19852				
T3	Excited State	3:	Triplet-A	4.1221 eV	300.78 nm	f=nd	$\langle S^{**2} \rangle = 2.000$
	60 -> 64		-0.41311				
	60 -> 66		-0.11005				
	61 -> 65		0.15395				
	63 -> 64		0.44410				
	63 -> 66		0.23257				
T4	Excited State	4:	Triplet-A	4.6260 eV	268.02 nm	f=nd	$\langle S^{**2} \rangle = 2.000$
	61 -> 64		0.49800				
	61 -> 65		0.11791				
	61 -> 66		-0.42177				
	63 -> 65		-0.10443				
T5	Excited State	5:	Triplet-A	4.6665 eV	265.69 nm	f=nd	$\langle S^{**2} \rangle = 2.000$
	60 -> 64		0.27244				
	60 -> 66		-0.10889				
	61 -> 65		0.49220				
	61 -> 66		0.13411				
	61 -> 67		-0.12576				
	61 -> 68		-0.13926				
	63 -> 64		0.16111				

63 -> 66	-0.24527					
T6 Excited State	6:	Triplet-A	4.8634 eV	254.93 nm	f=nd	<S**2>=2.000
59 -> 64	-0.12739					
60 -> 68	-0.37481					
62 -> 64	-0.31472					
63 -> 65	0.20280					
63 -> 68	0.38059					
T7 Excited State	7:	Triplet-A	4.9040 eV	252.83 nm	f=nd	<S**2>=2.000
60 -> 65	0.39016					
60 -> 67	-0.10349					
63 -> 65	0.46239					
63 -> 66	0.11803					
63 -> 67	-0.10697					
63 -> 68	-0.21121					
S1 Excited State	8:	Singlet-A	5.0626 eV	244.90 nm	f=0.4991	<S**2>=0.000
60 -> 64	-0.15113					
60 -> 66	-0.18343					
62 -> 68	-0.20813					
63 -> 64	0.60912					
T8 Excited State	9:	Triplet-A	5.1996 eV	238.45 nm	f=nd	<S**2>=2.000
52 -> 64	-0.10065					
56 -> 64	0.13488					
60 -> 66	-0.15474					
60 -> 70	0.10211					
62 -> 65	0.15934					
62 -> 68	0.54527					
63 -> 70	-0.15433					
63 -> 72	-0.15996					
S2 Excited State	10:	Singlet-A	5.3058 eV	233.68 nm	f=0.0056	<S**2>=0.000
60 -> 65	0.22786					
61 -> 64	0.41767					
61 -> 66	-0.31319					
62 -> 64	0.11152					
63 -> 65	0.33352					
T9 Excited State	11:	Triplet-A	5.3487 eV	231.80 nm	f=nd	<S**2>=2.000
59 -> 64	0.39323					
59 -> 72	0.12080					
60 -> 68	-0.15316					
62 -> 64	0.14717					
62 -> 66	-0.21286					
62 -> 70	0.28531					
62 -> 72	0.26152					
63 -> 68	0.16861					
S3 Excited State	12:	Singlet-A	5.5616 eV	222.93 nm	f=0.0891	<S**2>=0.000
60 -> 68	-0.14616					
61 -> 64	-0.11434					
62 -> 64	0.60870					
62 -> 66	0.19538					
63 -> 68	0.18833					
S4 Excited State	13:	Singlet-A	5.6397 eV	219.84 nm	f=0.1584	<S**2>=0.000
60 -> 64	0.45845					
61 -> 65	-0.16526					
62 -> 68	0.26787					
63 -> 64	0.23038					
63 -> 66	-0.29816					
T10 Excited State	14:	Triplet-A	5.7372 eV	216.10 nm	f=nd	<S**2>=2.000
56 -> 64	-0.15832					
60 -> 66	0.25802					
60 -> 70	-0.16405					

60 -> 72	-0.14077	
62 -> 65	0.10545	
62 -> 68	0.34632	
63 -> 66	-0.12914	
63 -> 70	0.27116	
63 -> 72	0.26967	
 T11 Excited State 15:	Triplet-A	6.2422 eV 198.62 nm f=nd <S**2>=2.000
52 -> 64	-0.10051	
54 -> 64	-0.11880	
60 -> 64	0.38809	
60 -> 66	0.13123	
60 -> 70	0.18612	
60 -> 72	0.22924	
63 -> 64	0.21992	
63 -> 66	0.30751	
63 -> 72	0.12214	
 S5 Excited State 16:	Singlet-A	6.4326 eV 192.74 nm f=0.4893 <S**2>=0.000
60 -> 66	0.21409	
61 -> 65	0.40050	
61 -> 66	0.10021	
61 -> 68	-0.13969	
62 -> 65	0.14969	
62 -> 68	0.25670	
63 -> 64	0.16511	
63 -> 66	0.13415	
63 -> 70	0.19251	
63 -> 72	0.20386	
 S6 Excited State 17:	Singlet-A	6.4929 eV 190.95 nm f=0.1580 <S**2>=0.000
60 -> 65	-0.22664	
61 -> 64	0.49325	
61 -> 72	0.10685	
63 -> 65	-0.37331	

**Table S4** First TD- $\omega$ B97X/6-311++G(d,p)  $S_0 \rightarrow S_n$  and  $S_0 \rightarrow T_n$  transitions computed on **1-OTf**.  
Excitation energies and oscillator strengths:

Excited State 1:	Triplet-A	3.3598 eV 369.03 nm f=0.0000 <S**2>=2.000
91 -> 101	0.18923	
91 -> 103	-0.11590	
91 -> 104	0.21650	
92 -> 101	-0.10335	
92 -> 102	0.25056	
92 -> 103	-0.14444	
95 -> 101	0.20504	
95 -> 104	-0.13334	
96 -> 101	0.34206	
96 -> 104	0.10388	
97 -> 101	-0.23870	
 Excited State 2:	Triplet-A	3.4663 eV 357.68 nm f=0.0000 <S**2>=2.000
91 -> 101	-0.16279	
92 -> 102	-0.15525	
95 -> 101	0.37136	
95 -> 104	-0.29652	
96 -> 101	-0.18054	
96 -> 107	-0.12768	
96 -> 109	0.14614	
97 -> 104	0.14081	
 Excited State 3:	Triplet-A	4.1181 eV 301.07 nm f=0.0000 <S**2>=2.000
91 -> 101	-0.25963	
92 -> 101	0.13106	

92 ->102	-0.16702
92 ->103	0.12427
96 ->101	0.43211
96 ->104	-0.27971
97 ->101	-0.15112
 Excited State 4:	Triplet-A
91 ->101	0.24954
91 ->104	0.13938
92 ->101	0.50215
92 ->102	-0.10276
92 ->104	0.28730
96 ->102	0.10285
 Excited State 5:	Triplet-A
91 ->101	-0.28886
91 ->102	0.17968
92 ->101	0.16817
92 ->102	0.39104
92 ->103	-0.28926
96 ->104	-0.20212
 Excited State 6:	Triplet-A
90 ->101	-0.20242
91 ->107	0.13125
91 ->109	-0.15502
95 ->101	-0.28257
96 ->107	-0.28882
96 ->109	0.31760
97 ->101	0.15729
97 ->109	-0.10634
 Excited State 7:	Triplet-A
91 ->102	0.38391
91 ->103	-0.25085
92 ->101	-0.15871
92 ->102	-0.12954
92 ->103	0.11624
96 ->102	0.33145
96 ->103	-0.21979
97 ->102	-0.15172
 Excited State 8:	Singlet-A
91 ->104	0.13640
95 ->107	0.12286
95 ->109	-0.13674
96 ->101	0.57351
96 ->104	-0.13447
97 ->101	-0.24825
 Excited State 9:	Triplet-A
90 ->101	0.14673
91 ->104	-0.12585
95 ->104	0.11175
95 ->107	0.28948
95 ->109	-0.37317
96 ->107	-0.14834
96 ->112	-0.10977
97 ->109	0.12138
 Excited State 10:	Triplet-A
90 ->101	-0.28695
91 ->107	-0.10702
91 ->109	0.12231
95 ->104	-0.16262
95 ->107	0.22798
95 ->109	-0.13795
95 ->112	0.15429

95 ->115	0.12239
96 ->107	0.16035
96 ->109	-0.20407
97 ->107	-0.14795
97 ->109	0.12313
 Excited State 11:	Singlet-A
91 ->101	0.18917
91 ->102	-0.24992
91 ->103	0.13838
92 ->101	0.40203
92 ->103	-0.11941
92 ->104	0.21532
95 ->101	0.14426
96 ->102	-0.24085
96 ->103	0.14760
97 ->102	0.10747
 Excited State 12:	Singlet-A
92 ->101	0.12175
95 ->101	-0.27256
95 ->104	0.11105
97 ->101	0.13443
100 ->101	0.56197
100 ->104	-0.10044
 Excited State 13:	Triplet-A
100 ->101	0.68068
100 ->104	-0.11702
 Excited State 14:	Singlet-A
95 ->101	0.42179
95 ->104	-0.16085
96 ->107	-0.10879
97 ->101	-0.25257
100 ->101	0.37729
 Excited State 15:	Triplet-A
85 ->101	0.11636
89 ->101	-0.10825
91 ->104	-0.18058
95 ->107	-0.19252
95 ->109	0.23531
96 ->104	0.20251
96 ->110	0.12956
96 ->111	0.11517
96 ->112	-0.23044
96 ->113	-0.10914
96 ->115	-0.19685
97 ->107	0.10210
 Excited State 16:	Singlet-A
91 ->101	0.40411
92 ->101	-0.18264
92 ->102	0.14325
95 ->101	-0.13069
95 ->107	-0.19139
95 ->109	0.19657
96 ->101	0.15443
96 ->104	0.26338
97 ->104	-0.12323
 Excited State 17:	Singlet-A
90 ->101	-0.12010
94 ->101	0.10390
95 ->101	0.22555
95 ->104	-0.12553
96 ->101	0.23960

```

97 ->101          0.49976
99 ->101          -0.20762

Excited State 18:      Triplet-A      6.4082 eV 193.48 nm f=0.0000 <S**2>=2.000
94 ->101          0.10482
95 ->101          0.26622
96 ->101          0.19064
97 ->101          0.49743
97 ->104          -0.14031
99 ->101          -0.26866

Excited State 19:      Singlet-A      6.4092 eV 193.45 nm f=0.5239 <S**2>=0.000
91 ->101          0.20984
91 ->104          0.14154
92 ->101          -0.15968
92 ->102          0.32037
92 ->103          -0.17073
95 ->107          0.21107
95 ->109          -0.22290
96 ->101          -0.15398
96 ->112          0.13113
96 ->115          0.11423
97 ->101          0.11547

Excited State 20:      Singlet-A      6.5707 eV 188.69 nm f=0.1430 <S**2>=0.000
91 ->101          0.18572
91 ->102          0.19210
91 ->103          -0.14440
92 ->101          0.31872
96 ->102          0.26413
96 ->103          -0.12187
97 ->102          -0.14547
99 ->101          0.39506

```

## 6 References

- S1 Riera-Galindo, S.; Orbelli Biroli, A.; Forni, A.; Puttisong, Y.; Tessore, F.; Pizzotti, M.; Pavlopoulou, E.; Solano, E.; Wang, S.; Wang, G.; et al. Impact of Singly Occupied Molecular Orbital Energy on the N-Doping Efficiency of Benzimidazole Derivatives. *ACS Appl. Mater. Interfaces* **2019**, *11* (41), 37981–37990.
- S2 G. M. Sheldrick, *Acta Crystallogr. C Struct. Chem.* 2015, **71**, 3.
- S3 J.-D. Chai and M. Head-Gordon, *J. Chem. Phys.*, 2008, **128**, 084106.
- S4 Gaussian 16, Revision A.03, M. J. Frisch, G. W. Trucks, H. B. Schlegel, G. E. Scuseria, M. A. Robb, J. R. Cheeseman, G. Scalmani, V. Barone, G. A. Petersson, H. Nakatsuji, X. Li, M. Caricato, A. V. Marenich, J. Bloino, B. G. Janesko, R. Gomperts, B. Mennucci, H. P. Hratchian, J. V. Ortiz, A. F. Izmaylov, J. L. Sonnenberg, D. Williams-Young, F. Ding, F. Lipparini, F. Egidi, J. Goings, B. Peng, A. Petrone, T. Henderson, D. Ranasinghe, V. G. Zakrzewski, J. Gao, N. Rega, G. Zheng, W. Liang, M. Hada, M. Ehara, K. Toyota, R. Fukuda, J. Hasegawa, M. Ishida, T. Nakajima, Y. Honda, O. Kitao, H. Nakai, T. Vreven, K. Throssell, J. A. Montgomery, Jr., J. E. Peralta, F. Ogliaro, M. J. Bearpark, J. J. Heyd, E. N. Brothers, K. N. Kudin, V. N. Staroverov, T. A. Keith, R. Kobayashi, J. Normand, K. Raghavachari, A. P. Rendell, J. C. Burant, S. S. Iyengar, J. Tomasi, M. Cossi, J. M. Millam, M. Klene, C. Adamo, R. Cammi, J. W. Ochterski, R. L. Martin, K. Morokuma, O. Farkas, J. B. Foresman and D. J. Fox, Gaussian, Inc., Wallingford CT, 2016.